Cancer Letters 433 (2018) 18–32

Contents lists available at ScienceDirect

Cancer Letters

journal homepage: www.elsevier.com/locate/canlet

Original Articles

Agave negatively regulates YAP and TAZ transcriptionally and post-translationally in osteosarcoma cell lines

Maria Ferraiuolo[a,1], Claudio Pulito[a,1], Megan Finch-Edmondson[b], Etleva Korita[a], Anna Maidecchi[c], Sara Donzelli[a], Paola Muti[d], Massimo Serra[e], Marius Sudol[b,f,g,h], Sabrina Strano[a,*], Giovanni Blandino[a,**]

[a] Oncogenomic and Epigenetic Unit, Molecular Chemoprevention Group, Department of Research, Diagnosis and Innovative Technologies, Translational Research Area, Regina Elena National Cancer Institute, Rome, Italy
[b] The Mechanobiology Institute (MBI) and the NUS Yong Loo Lin School of Medicine, National University of Singapore, Republic of Singapore
[c] Aboca SpA Società Agricola, Sansepolcro, Italy
[d] Department of Oncology, Juravinski Cancer Center, McMaster University, Hamilton, Canada
[e] Laboratory of Experimental Oncology, Pharmacogenomics and Pharmacogenetics Research Unit, Orthopaedic Rizzoli Institute, Bologna, Italy
[f] Department of Physiology, Yong Loo Lin School of Medicine, National University of Singapore, Singapore
[g] Institute of Molecular and Cell Biology (IMCB), Agency for Science, Technology and Research (A*STAR), Singapore
[h] Mechanobiology Institute, National University of Singapore, Republic of Singapore

ARTICLE INFO

Keywords:
Agave
Osteosarcoma
Saponins
YAP/TAZ
Proliferation

ABSTRACT

Osteosarcoma (OS) is the most aggressive type of primary solid tumor that develops in bone. Whilst conventional chemotherapy can improve survival rates, the outcome for patients with metastatic or recurrent OS remains poor, so novel treatment agents and strategies are required. Research into new anticancer therapies has paved the way for the utilisation of natural compounds as they are typically less expensive and less toxic compared to conventional chemotherapeutics. Previously published works indicate that Agave exhibits anticancer properties, however potential molecular mechanisms remain poorly understood. In the present study, we investigate the anticancer effects of Agave leaf extract in OS cells suggesting that Agave inhibits cell viability, colony formation, and cell migration, and can induce apoptosis in OS cell lines. Moreover, Agave sensitizes OS cells to cisplatin (CDDP) and radiation, to overcome chemo- and radio-resistance. We demonstrate that Agave extract induces a marked decrease of Yes Associated Protein (YAP) and Tafazzin (TAZ) mRNA and protein expression upon treatment. We propose an initial mechanism of action in which Agave induces YAP/TAZ protein degradation, followed by a secondary event whereby Agave inhibits YAP/TAZ transcription, effectively deregulating the Nuclear Factor kappa B (NF-κB) p65:p50 heterodimers responsible for transcriptional induction of YAP and TAZ.

1. Introduction

Osteosarcoma (OS) is the most frequent primary tumor affecting bone, and typically originates in the extremities of the long bones in the legs. It is always associated with increasing pain [1,2]. OS shows a bimodal age occurrence, arising frequently in children and teens aged 10–16 years, and in older adults usually over 40. Neoplastic cells show a complex karyotype associated with chromosome instability, copy number variation and deregulation of many signalling pathways such as Vascular Endothelial Growth Factor-Receptor (VEGF-R), Transforming Growth Factor-beta (TGFβ), Wnt/β-catenin, Hippo/YAP, Hedgehog, Notch and PI3K-Akt-mTOR [3,4]. First line treatment is intravenous combinational chemotherapy (cisplatin (CDDP)/doxorubicin) [3]. For patients with localized OS, surgical resection is an essential component of the therapy, however if not feasible, radiation therapy can be used to improve prognosis [5,6]. OS is frequently associated with chemo- and

Abbreviations: Cisplatin, CDDP; Cycloheximide, CHX; Epithelial to mesenchymal transition, EMT; Nuclear Factor kappa-light-chain-enhancer of activated B cells, NF-κB; Osteosarcoma, OS; half-maximal effective concentration, EC50; half-maximal lethal concentration, LC50; cocktail protein inhibitors, CI; 4′, 6-diamidino-2- phenylindole, DAPI

* Corresponding author. Oncogenomic and Epigenetic Unit, Molecular Chemoprevention Group, Department of Research, Diagnosis and Innovative Technologies, Translational Research Area Regina Elena National Cancer Institute, Via Elio Chianesi, 53, 00144, Roma, Italy.
** Corresponding author. Oncogenomic and Epigenetic Unit, Department of Research, Diagnosis and Innovative Technologies, Translational Research Area Regina Elena National Cancer Institute, Via Elio Chianesi, 53, 00144, Roma, Italy.
E-mail addresses: sabrina.strano@ifo.gov.it (S. Strano), giovanni.blandino@ifo.gov.it (G. Blandino).
[1] These authors contribute equally to the work.

https://doi.org/10.1016/j.canlet.2018.06.021
Received 24 December 2017; Received in revised form 1 June 2018; Accepted 14 June 2018

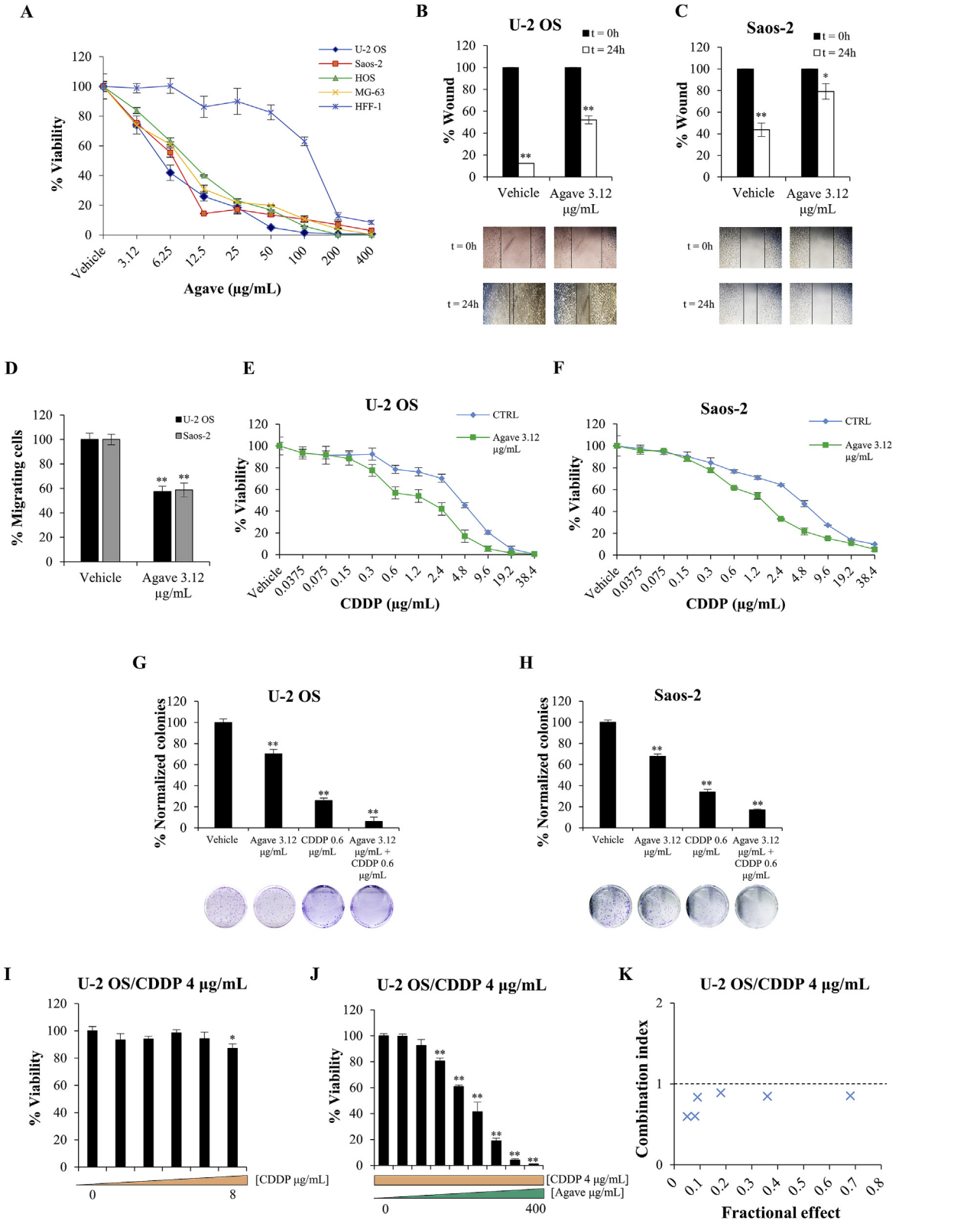

(caption on next page)

radio-resistance due to the presence of cancer stem cell subpopulations and Hippo/YAP signalling alterations [3,7]. The five-year survival rate for patients with metastatic or recurrent disease has essentially remained unchanged at approximately 20% [8,9]. New, effective OS anticancer strategies are urgently required, paving the way for research into less-toxic, cost-effective natural compounds that could be useful as novel OS therapeutics.

The Hippo pathway is an evolutionarily conserved signalling pathway that plays a key role in development, stem cell maintenance, regeneration, cancer onset, and chemoresistance [7,10–12]. The Hippo core comprises the Lats1/2-(Mob1-Sav1)-Mst1/2 protein kinases that function as tumor suppressors. The core kinase cassette induces

Fig. 1. Agave exerts anticancer effects on osteosarcoma cell lines. **(A)** Osteosarcoma cell lines were treated with Vehicle control (EtOH) or increasing concentrations of Agave for 72 h before being analyzed by ATPlite assay. The percentage cell viability normalized to control is shown, with values representing mean ± STDEV of n = 3 independent experiments. Wound healing- **(B–C)** and transwell- **(D)** migration assays were performed on U-2 OS (B, D) and Saos-2 (C, D) cell lines after treatment with Agave (3.12 μg/mL) or Vehicle for 24 h. Histograms represent the percentage of wound width (B–C) or migrated cells (D) normalized to the relevant controls. Values represent mean ± STDEV from n = 3 independent experiments, *p < 0.01 **p < 0.001. Osteosarcoma cell lines U-2 OS **(E)** and Saos-2 **(F)** were treated with either Vehicle (CTRL) or Agave (3.12 μg/mL) in combination with increasing doses of cisplatin (CDDP) for 72 h. The percentage viability of Agave treatment alone was subtracted from each CDDP or CTRL value (corrected value), then these data were normalized to the CTRL corrected value. Values shown represent mean ± STDEV from n = 3 independent experiments. U-2 OS **(G)** and Saos-2 **(H)** cell lines were treated with Vehicle, Agave (3.12 μg/mL), and/or CDDP (0.6 μg/mL) for 24 h after seeding for clonogenic assays. Histograms represent the mean percentage of colonies ± STDEV normalized to Vehicle control from n = 3 independent experiments, ANOVA **p < 0.001. Images underneath histograms are representative stained culture dishes used for counting colonies. U-2 OS/CDDP 4 μg/mL cell line was treated with increasing concentrations of CDDP **(I)** or Agave with a fixed dose of CDDP (4 μg/mL) **(J)** for 72 h before being analyzed by ATPlite assay. Histograms represent the percentage of cell viability normalized to control, with values representing mean ± STDEV of n = 3 independent experiments, ANOVA *p < 0.01 **p < 0.001. **(K)** Combination index versus the fractional effect obtained from U-2 OS/CDDP 4 μg/mL cells pretreated with Agave extract (3.12 μg/mL) for 24 h and subsequently with CDDP (1–8 μg/mL) for 72 h. Combination index was calculated using Calcusyn software.

Table 1
Treatment with Agave reduces cell viability. The half-maximal effective concentration (EC50) and the half-maximal lethal concentration (LC50) values for osteosarcoma and HFF-1 cell lines treated with Agave, calculated using Compusyn software from the dose-response curves in Fig. 1A.

Phytocompound Agave treatments									
U-2 OS		Saos-2		HOS		MG-63		HFF-1	
EC50 (μg/mL)	LC50 (μg/mL)	EC50 (μg/mL)	LC50 (μg/mL)	EC50 (μg/mL)	LC50 (μg/mL)	EC50 (μg/mL)	LC50 (μg/mL)	EC50 (μg/mL)	LC50 (μg/mL)
3.67	5.21	4.8	6.3	6.16	9.38	4.39	7.81	159.03	116.67

Table 2
Agave sensitizes osteosarcoma cells to cisplatin. The half-maximal effective concentration (EC50) and the half-maximal lethal concentration (LC50) values for osteosarcoma cell lines treated with cisplatin (CDDP) in combination with Agave (3.12 μg/mL) or EtOH control (CTRL), calculated using Compusyn software from the dose-response curves in Fig. 1E–F.

Samples	U-2 OS		Saos-2	
	CDDP EC50 (μg/mL)	CDDP LC50 (μg/mL)	CDDP EC50 (μg/mL)	CDDP LC50 (μg/mL)
CTRL	1.66	4.4	2.89	4.4
Agave 3.12 μg/mL	0.76	1.5	1.4	1.5

Table 3
Agave sensitizes U-2 OS CDDP resistant cell line to cisplatin. The half-maximal effective concentration (EC50) and the half-maximal lethal concentration (LC50) values for U-2 OS/CDDP 4 μg/mL osteosarcoma cell line treated with increased doses of cisplatin (CDDP) or Agave, calculated using Compusyn software from the dose-response curves in Fig. 1I–J.

Cell line	CDDP EC50 (μg/mL)	CDDP LC50 (μg/mL)	Agave EC50 (μg/mL)	Agave LC50 (μg/mL)
U-2 OS/CDDP 4 μg/mL	> 32	26.67	50.73	37.5

phosphorylation of the oncogenic Hippo transducers YAP and TAZ resulting in their cytoplasmic retention and/or protein degradation [13]. Since YAP and TAZ lack a DNA binding domain, they interact with various DNA-binding transcription factors including TEADs/TEFs, β-catenin, RUNX1/2 and Smads to drive transcription of their oncogenic target genes. Interestingly, the Hippo pathway has been shown to cooperate with p53 signalling to induce apoptosis, DNA damage repair, and senescence [14].

The NF-κB family of transcription factors are key regulators of immune development, immune responses, inflammation, and cancer [15]. In the absence of stimuli, NF-κB is inactivated and sequestered in the cytoplasm through binding to the inhibitor protein IκBα; in the presence of stimuli, the activated kinase IKK phosphorylates IκBα, promoting its proteasomal degradation and NF-κB release. Thus, activated NF-κB translocates into the nucleus to promote transcription of its target genes [15]. NF-κB acts as dimer of different subunits: p65 (or RelA), RelB, p50 (obtained from p105 precursor), p52 (produced from p100 precursor), and cRel.

In the present study, we observe that Agave natural extract inhibits the survival and migration of OS cell lines, and sensitizes them to CDDP and radiation treatments. We demonstrate that Agave mediates its anticancer activity via increasing YAP and TAZ protein degradation, and subsequently inhibiting the formation of NF-κB p65:p50 pro-transcriptional heterodimers. These results suggest that targeting the Hippo pathway may be an effective strategy to treat OS.

2. Materials and methods

2.1. Cell culture and reagents

Cell lines HFF-1, U-2 OS, Saos-2, HOS, MG-63, H1299, A549, MDA-MB-231, SUM-159PT, MSTO-211H and MPP-89 were obtained from the ATCC (Manassas, US) and cultured accordingly. Tumoural cell lines were checked and tested for p53 status. Specifically, we used wt-p53 cell lines (U-2 OS, A549, MSTO-211H, MPP-89), mutant p53 (HOS, MDA-MB-231, SUM-159PT) and p53-null cells (Saos-2, MG-63, H1299). U-2 OS cell line resistant to Cisplatin (CDDP) 4 μg/mL (U-2 OS/CDDP 4 μg/mL) was provided by “Laboratory of Experimental Oncology” from the “Rizzoli Orthopedic Institute” [16] and cultured in Iscoves's modified Dulbecco's Medium (IMDM; Life Technologies, California, USA) 10% FBS supplemented with CDDP 4 μg/mL. Agave total extract from frozen leaf samples of *Agave sisalana* plant was provided in powder and characterized as previously described from the Italian Aboca Society [17]. Saponins Diosgenin (Cat. D1634), Sarsasapogenin (Cat. S8534) and Solasodine (Cat. SML1141) were purchased from Sigma (Saint Louis, Missouri, US). Cisplatin (CDDP), doxorubicin, methotrexate and isofosfamide were provided by the Pharmacy of the “Regina Elena National Cancer Institute” in Rome. DAPI (4′, 6-diamidino-2- phenylindole, dihydrochloride, Sigma Cat. 32670) was used to stain cell nuclei. Protease Inhibitor Cocktail (CI) (Cat. P8340), MG-132 (Z-Leu-Leu-Leu-al, Cat. C2211), cycloheximide (CHX) (Cat. 01810), IL-6 (Cat. I1395), verteporfin (Cat. SML0534), dasatinib (Cat. CDS023389) and pazopanib (Cat. CDS023580) were purchased from Sigma.

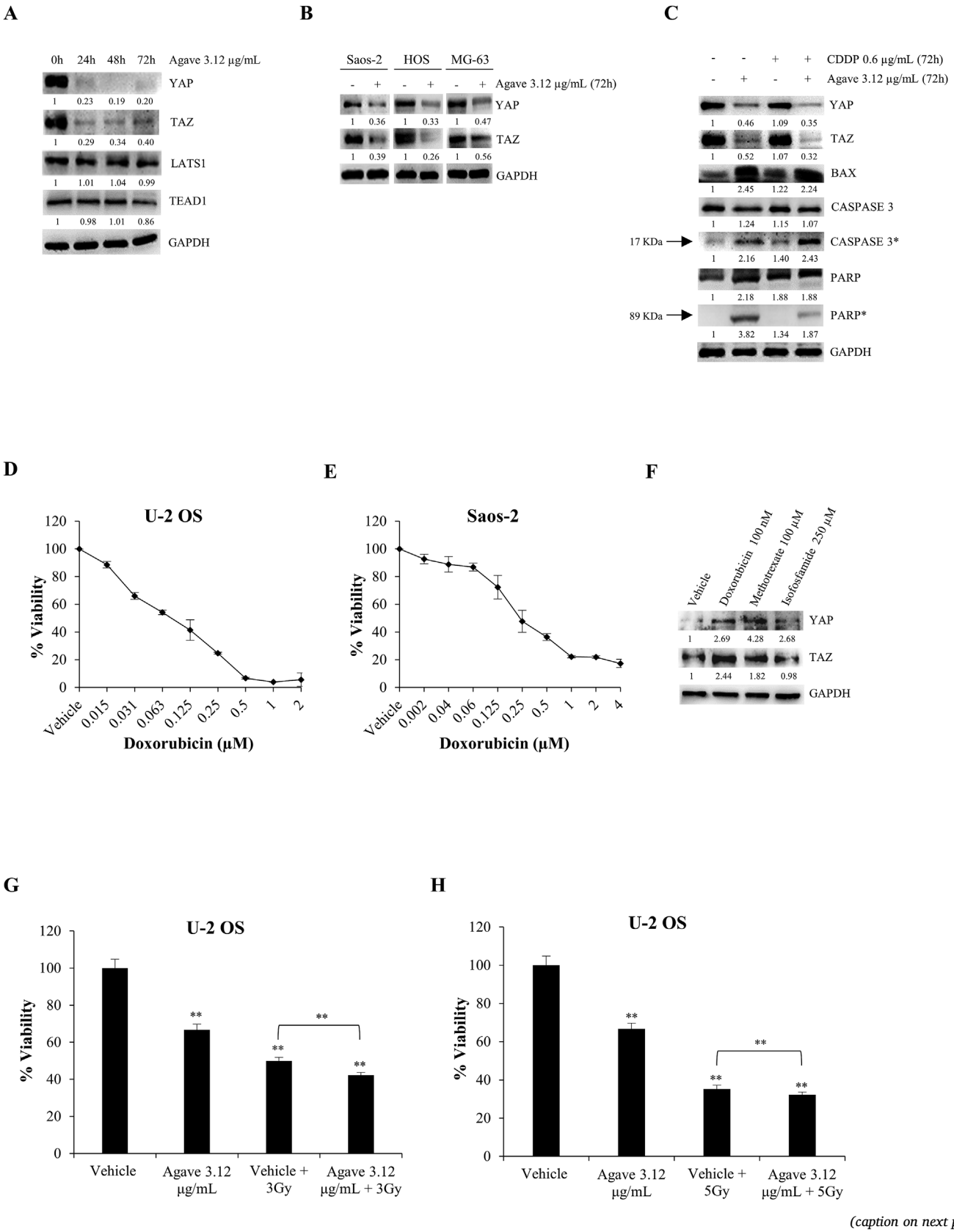

(caption on next page)

2.2. Cell transfection

Transfections were performed using Lipofectamine 2000 (for plasmids) and Lipofectamine RNAiMax (for siRNA) (Life Technologies) according to the manufacturer's recommendations.

siRNAs were purchased from Eurofins MWG (Ebersberg, Germany): siGFP [18], siYAP [19], siTAZ is a pool of two independent siRNAs mixed in equal amount [20]. To exclude unspecific effects, we

Fig. 2. Agave sensitizes osteosarcoma cells to chemo- and radio-therapy by down-regulating YAP and TAZ. **(A)** U-2 OS cells were treated with Agave (3.12 μg/mL) for 24, 48 or 72 h, or EtOH as Vehicle control (0 h), then subjected to Western Blot analysis as indicated. GAPDH was used as a loading control. Numbers underneath immunoblots represent normalized protein amount quantified using Alliance (UVITEC) Software. Values shown are representative from n = 3 independent experiments. **(B)** Saos-2, HOS and MG-63 cell lines were treated with Agave (3.12 μg/mL) or Vehicle for 72 h, and **(C)** U-2 OS cells were treated with Vehicle, Agave (3.12 μg/mL) and/or CDDP (0.6 μg/mL) for 72 h before being subjected to Western Blot analysis as indicated. GAPDH was used as a loading control. Numbers underneath immunoblots represent normalized protein amount quantified using Alliance (UVITEC) Software. Values shown are representative from n = 3 independent experiments. U-2 OS **(D)** and Saos-2 **(E)** were treated with Vehicle control (DMSO) or increasing concentrations of doxorubicin for 72 h before being analyzed by ATPlite assay. The percentage cell viability normalized to control is shown, with values representing mean ± STDEV of n = 3 independent experiments. **(F)** U-2 OS cells were treated with Vehicle control (DMSO), doxorubicin (100 nM), methotrexate (100 μM) or isofosfamide (250 μM) for 72 h before being subjected to Western Blot analysis as indicated. GAPDH was used as a loading control. Numbers underneath immunoblots represent normalized protein amount quantified using Alliance (UVITEC) Software. Values shown are representative from n = 3 independent experiments. U-2 OS cells were pre-treated with Vehicle control (EtOH) or Agave (3.12 μg/mL) before being subjected to Cs^{137} γ-irradiation reaching a 3Gy **(G)** or 5Gy **(H)** cumulative dose. ATPlite assay was performed after 72 h and the percentage cell viability, normalized to control, is shown in histograms, with values representing mean ± STDEV of n = 3 independent experiments, ANOVA $^{**}p < 0.001$.

Table 4
Doxorubicin treatments in OS cell lines. The half-maximal effective concentration (EC50) and the half-maximal lethal concentration (LC50) values for U-2 OS and Saos-2 osteosarcoma cell line treated with increased doses of Doxorubicin (Doxo), calculated using Compusyn software from the dose-response curves in Fig. 2D–E.

Cell line	Doxo EC50 (μM)	Doxo LC50 (μM)
U-2 OS	0.096	0.084
Saos-2	0.322	0.232

previously performed YAP and TAZ silencing with two different siRNAs. Representative data are showed in figures. Plasmids utilized were: pCDNA3-YAP-Flag [21], pCS2-TAZ-Flag [22], and pCS2-Ub-HA [23].

2.3. Viability, clonogenic, and wound healing migration assays

Viability, clonogenic and wound healing migration assays were performed as previously described [24].

2.4. Radiation treatments

A number of 2×10^5 cells was plated in 60 mm plates and treated after 24 h as indicated. The day after, cells were placed in an irradiation chamber and subjected to 0.08 Gy/min Cs^{137} γ-irradiation for 37.5 s and for 62.5 s. This allowed obtaining 3Gy and 5Gy cumulative doses, respectively. After additional 24 h, cells were detached and plated in 96-well (1500 cells per well). ATPlite assay (Perkin Elmer, Massachusetts, USA) was performed after 72 h as previously described [24].

2.5. Cell extracts, immunoprecipitation and Western Blotting

Cell lysis, protein quantification, Immunoprecipitation (IP) and Western Blot analysis were performed as previously described [24]. Primary antibodies are listed in Supplementary Table S2.

2.6. RNA extraction, reverse transcription and quantitative Real-Time PCR

RNA was extracted, reverse-transcribed and subjected to quantitative Real-Time PCR (qPCR) as previously described [25]. Data were analyzed using the relative standard curve method and normalized to GAPDH. Primer sequences are listed in Supplementary Table S3.

2.7. Protein stability assay

Cells were treated with Vehicle or Agave as indicated and simultaneously treated with cycloheximide (CHX) 40 μM for the indicated times. Cells were subsequently lysed and subjected to Western Blotting as previously described.

2.8. Ubiquitination assay

A number of 1.6×10^6 cells was transfected with the indicated plasmids as previously described and simultaneously treated as indicated. After 18 h, cells were treated with 25 μM MG-132 for a further 6 h. Protein extracts were immunoprecipitated as described and subjected to Western Blotting. Antibody details are listed in Supplementary Table S2.

2.9. Nuclear/cytoplasmic protein extraction

Nuclear/cytoplasmic protein extraction was performed as previously described [26]. Refer to Supplementary Table S2 for antibody specifications.

2.10. Immunofluorescent staining

Cells were processed as previously described [17] and treated as indicated for 72 h. IL-6 treatments were performed using 100 ng/mL for 30 min before recovering cells. Antibodies specifications are listed in Supplementary Table S2.

2.11. Chromatin immunoprecipitation assay (ChIP)

ChIP assays were performed and data were analyzed as previously reported [20]. Refer to Supplementary Table S2 for antibody specifications. Primer sequences are listed in Supplementary Table S3.

2.12. Promoter analysis

FASTA sequences of human YAP1 (NM_001130145) and WWTR1 (TAZ) (NM_015472) promoters (4000 bp upstream of the TSS) were downloaded from UCSC Genome Browser on-line database and pasted into LASAGNA-Search 2.0 to identify predicted transcription factor binding sites. TRANSFAC matrices were used for the analysis.

2.13. Statistical analyses

All experiments were performed at least three independent times and the most representative results are shown. No samples were excluded from the analysis. For statistical analysis, we used two-tailed t-tests for comparison analysis between two populations, and the F-test ANOVA and the post-hoc Tukey test for multiple comparisons analysis. All p-values were determined and statistical significance was set at $^{*}p < 0.01$, $^{**}p < 0.001$.

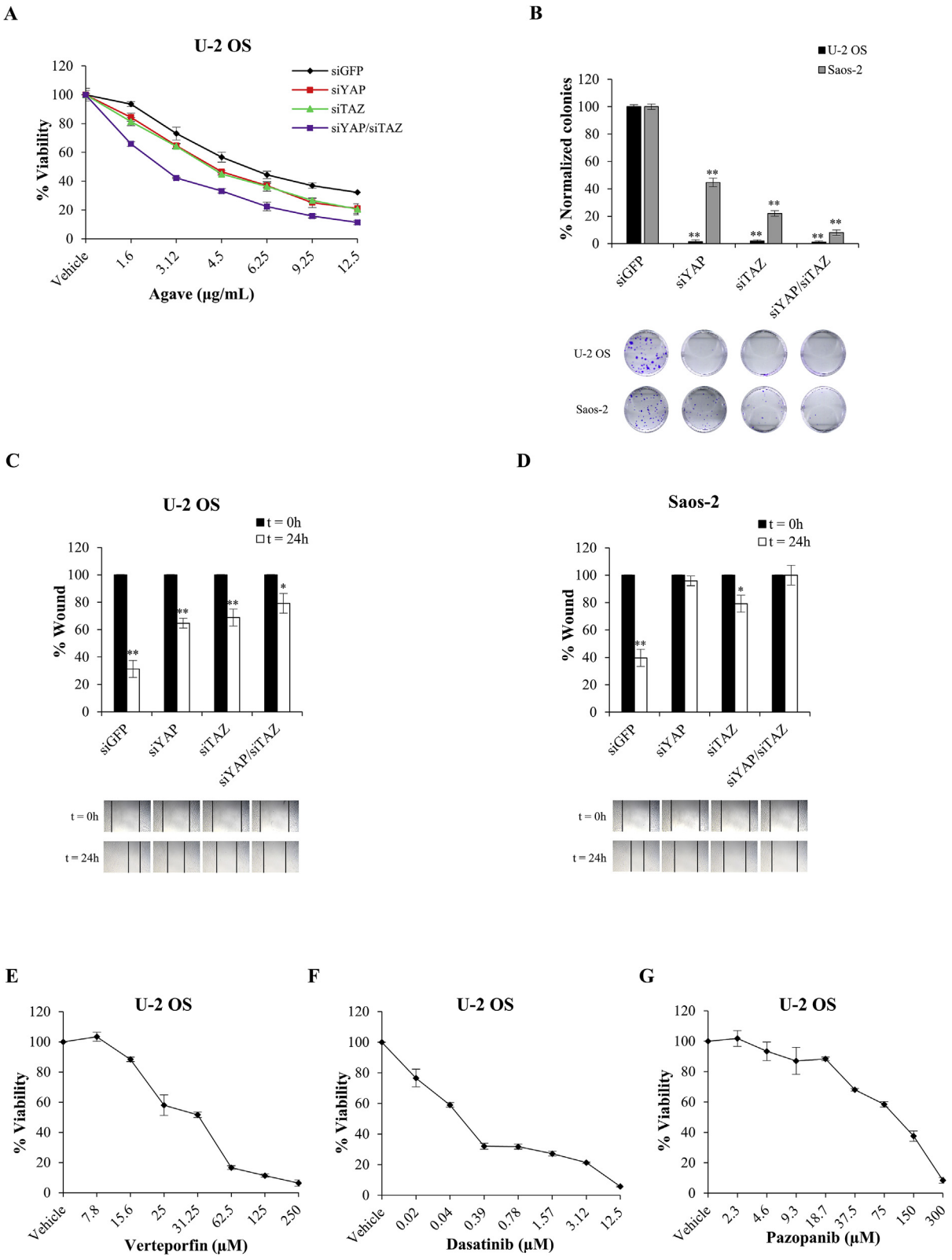

Fig. 3. Down-regulation of YAP and TAZ oncogenes sensitizes cells to Agave treatments. **(A)** U-2 OS cells transfected with siGFP (control), siYAP, siTAZ or siYAP/siTAZ were treated with increasing doses of Agave diluted in Vehicle. Values represent the mean percentage viability ± STDEV for each condition (n = 3), determined by ATPlite assay. **(B)** U-2 OS and Saos-2 cells were transfected with siGFP (control), siYAP, siTAZ or siYAP/siTAZ and subjected to clonogenic assays. Histograms show the mean percentage of colonies ± STDEV normalized to siGFP from n = 3 independent experiments, ANOVA **p < 0.001. Images underneath histograms are representative stained culture dishes used for counting colonies. U-2 OS **(C)** and Saos-2 **(D)** cells were transfected with siGFP (control), siYAP, siTAZ or siYAP/siTAZ and subjected to wound healing assays. Histograms show the mean percentage of wound width ± STDEV normalized to siGFP from n = 3 independent experiments, ANOVA *p < 0.01 **p < 0.001. Images underneath histograms are representative of the wounded areas used for measuring wound opening. U-2 OS cells were treated with Vehicle control or increasing concentrations of YAP/TAZ inhibitors verteporfin **(E)**, dasatinib **(F)** or pazopanib **(G)** for 72 h before being analyzed by ATPlite assay. The percentage cell viability normalized to control is shown, with values representing mean ± STDEV of n = 3 independent experiments.

Table 5
YAP and TAZ depletion sensitizes osteosarcoma cells to Agave. The half-maximal effective concentration (EC50) and the half-maximal lethal concentration (LC50) values for Agave treatment of siGFP (control), siYAP, siTAZ, or siYAP/siTAZ U-2 OS cell lines, analyzed using Compusyn software from the dose-response curves in Fig. 3A.

Samples	Agave	Agave
	EC50 (μg/mL)	LC50 (μg/mL)
siGFP	7.6	5.2
siYAP	4	4
siTAZ	3.8	4
siYAP/siTAZ	1.8	2.4

Table 6
YAP and TAZ inhibitors reduce osteosarcoma cell viability. The half-maximal effective concentration (EC50) and the half-maximal lethal concentration (LC50) values for U-2 OS and Saos-2 cells treated with the YAP/TAZ inhibitors verteporfin, dasatinib and pazopanib, calculated using Compusyn software from the dose-response curves in Fig. 3E–G and Supplementary Figs. S2C–E.

Synthetic compounds	U-2 OS		Saos-2	
	EC50 (μM)	LC50 (μM)	EC50 (μM)	LC50 (μM)
Verteporfin	39.45	31.25	19.93	15.58
Dasatinib	0.174	0.127	1.12	1.54
Pazopanib	46.85	105	49.8	31.25

3. Results

3.1. Agave reduces cell viability, colony formation, cell migration, and sensitizes cells to CDDP

Searching for potential alternate OS therapeutics, we performed cell viability assays testing 15 natural compounds on U-2 OS and Saos-2 OS cell lines (data not shown). We noted that of the 15 compounds tested, Agave natural extract showed the greatest reduction in cell viability. We therefore focused on this extract and extended our analysis to four OS cell lines: U-2 OS, Saos-2, HOS and MG-63. Dose-response assays were performed using Agave treatment for 72 h (Fig. 1A). Table 1 shows the half-maximal effective concentration (EC50) and the half-maximal lethal concentration (LC50) for each cell line. EC50 values ranged from 3.67 μg/mL in U-2 OS to 6.16 μg/mL in HOS cells (Table 1). Interestingly, we found that Agave-induced killing effect was more effective toward cancer cells. Indeed, human fibroblast HFF-1 cells resulted more resistant (EC50 159.03 μg/mL) than OS cells in response to Agave treatments; thereby suggesting that Agave is not toxic for normal cells, at least, for the amounts inducing OS cell death (Fig. 1A and Table 1). For subsequent functional analyses, we selected the lower dose of Agave 3.12 μg/mL, which reduced cell viability by approximately 25% (Fig. 1A). We tested cell migratory ability after 24 h of Agave treatment using wound healing- (Fig. 1B–C) and transwell- (Fig. 1D) migration assays, and found that Agave impairs cell migration in both U-2 OS and Saos-2 cell lines.

The biggest challenge in OS therapy is overcoming chemoresistance [3]. To determine whether Agave can improve the effectiveness of CDDP as an apoptotic agent, we assayed Agave in combination with increasing doses of CDDP for 72 h (Fig. 1E–F). Agave extract sensitized OS cells to CDDP, effectively reducing the EC50 (by 2.2-fold) and LC50 (by 2.9-fold) for U-2 OS and Saos-2 cells (Table 2). Clonogenic assays were then performed to assess colony formation ability using U-2 OS and Saos-2 cell lines treated with Agave and CDDP either alone or in combination (Fig. 1G–H). Whilst CDDP was more effective than Agave in reducing colony numbers, Agave potentiated CDDP's inhibitory effect in both cell lines. To test whether Agave treatment could overcome chemoresistance to conventional OS treatments, we assayed the ability of Agave to promote cell death of a CDDP-resistant OS cell line. To this end, U-2 OS/CDDP 4 μg/mL cells were treated with increasing doses of CDDP (Fig. 1I and Table 3) and Agave (Fig. 1J and Table 3) for 72 h. Notably, we found that unlike CDDP, Agave promoted cell death of U-2 OS/CDDP 4 μg/mL cells and had additive and synergistic effect with CDDP in reducing OS cell viability (Fig. 1K).

Agave's inhibitory effect on cell viability was also tested in a variety of other cancer cell lines (lung, mesothelioma and breast) (Supplementary Fig. S1) demonstrating a consistent dose-dependent effect.

3.2. Agave decreases oncogenic YAP and TAZ protein levels and induces apoptosis

As previously described, OS typically exhibits dysregulation of multiple signalling pathways, including Hippo/YAP [4]. Alterations in this pathway have also been demonstrated to be a driver of chemo- and radio-resistance in OS patients [7]. To determine the mechanism of Agave's anticancer effects we investigated different signalling pathways and focused on alterations within the Hippo pathway, specifically the Hippo transducers YAP and TAZ. Agave decreased YAP and TAZ protein expression after 24 h in U-2 OS cells (Fig. 2A). Notably, Lats1 protein level was unchanged, and TEA Domain transcription factor 1 (TEAD1) only mildly down-regulated after 72 h of Agave treatment. Reduced YAP and TAZ expression was also observed in Saos-2, HOS and MG-63 lines after 72 h of Agave treatment (Fig. 2B). Treatment with CDDP alone did not affect YAP and TAZ protein levels (Fig. 2C). Moreover, Agave induced apoptosis by increasing Bax protein expression, as well as Caspase 3 and PARP cleavage (lanes 1–2, Fig. 2C), this effect is stronger compared to that mediated by CDDP treatment alone (lanes 1 and 3, Fig. 2C), and appears to enhance CDDP's effect increasing Caspase 3 cleavage in combined treatment (lanes 3–4, Fig. 2C). Conventional OS therapies comprise also combined treatments with doxorubicin, methotrexate and isofosfamide [3]. We tested doxorubicin effect on U-2 OS and Saos-2 treated cells for 72 h (Fig. 2D–E) calculating EC50 and LC50 for each cell line (Table 4), then we selected the dose of 100 nM to test YAP and TAZ protein expression (Fig. 2F). We found that doxorubicin treatment for 72 h induced YAP and TAZ protein levels in U-2 OS cell line supporting previous published results [7]. Treatment with methotrexate 100 μM for 72 h, induced YAP and TAZ as well, whereas isofosfamide 250 μM induced YAP upregulation but not TAZ modulation after 72 h of treatment (Fig. 2F). We also found that Agave improved the killing effects of radiotherapy, when used (3.12 μg/mL) in combination with 3Gy or 5Gy of Cs^{137} γ-radiation. Agave extract sensitized OS cells to radiation, effectively reducing cell viability compared to the irradiated samples alone (Fig. 2G–H).

These data suggest that Agave reduces cell viability and sensitizes OS cells to chemo- and radio-therapy by down-regulating YAP and TAZ that are known to function as oncogenes in OS cells [4,7]. Indeed, YAP/TAZ silencing sensitized OS cell lines to Agave (Fig. 3A), reducing the EC50 and LC50 concentrations by 4.2- and 2.2-fold, respectively (Table 5). Moreover, silencing of YAP and TAZ reduced the clonogenic and migratory capabilities of both U-2 OS and Saos-2 cell lines (Fig. 3B–D and Supplementary Figs. S2A–B). Among FDA-approved YAP and TAZ inhibitors, stand out verteporfin, dasatinib and pazopanib [27,28]. To confirm that YAP and TAZ exert an oncogenic crucial role in OS cell survival, we assayed U-2 OS and Saos-2 cell lines with increased doses of verteporfin (Fig. 3E and Supplementary Fig. S2C), dasatinib (Fig. 3F and Supplementary Fig. S2D) and pazopanib (Fig. 3G and Supplementary Fig. S2E) and we calculated the EC50 and LC50 for each synthetic compound in both cell lines (Table 6). We found that the YAP/TAZ inhibitors significantly reduced OS cells viability in a dose-dependent manner. Altogether these findings mirror an important role of YAP and TAZ in the chemoresistance of osteosarcoma cells thereby suggesting YAP/TAZ targeting as a therapeutic approach to improve the outcome of OS patients.

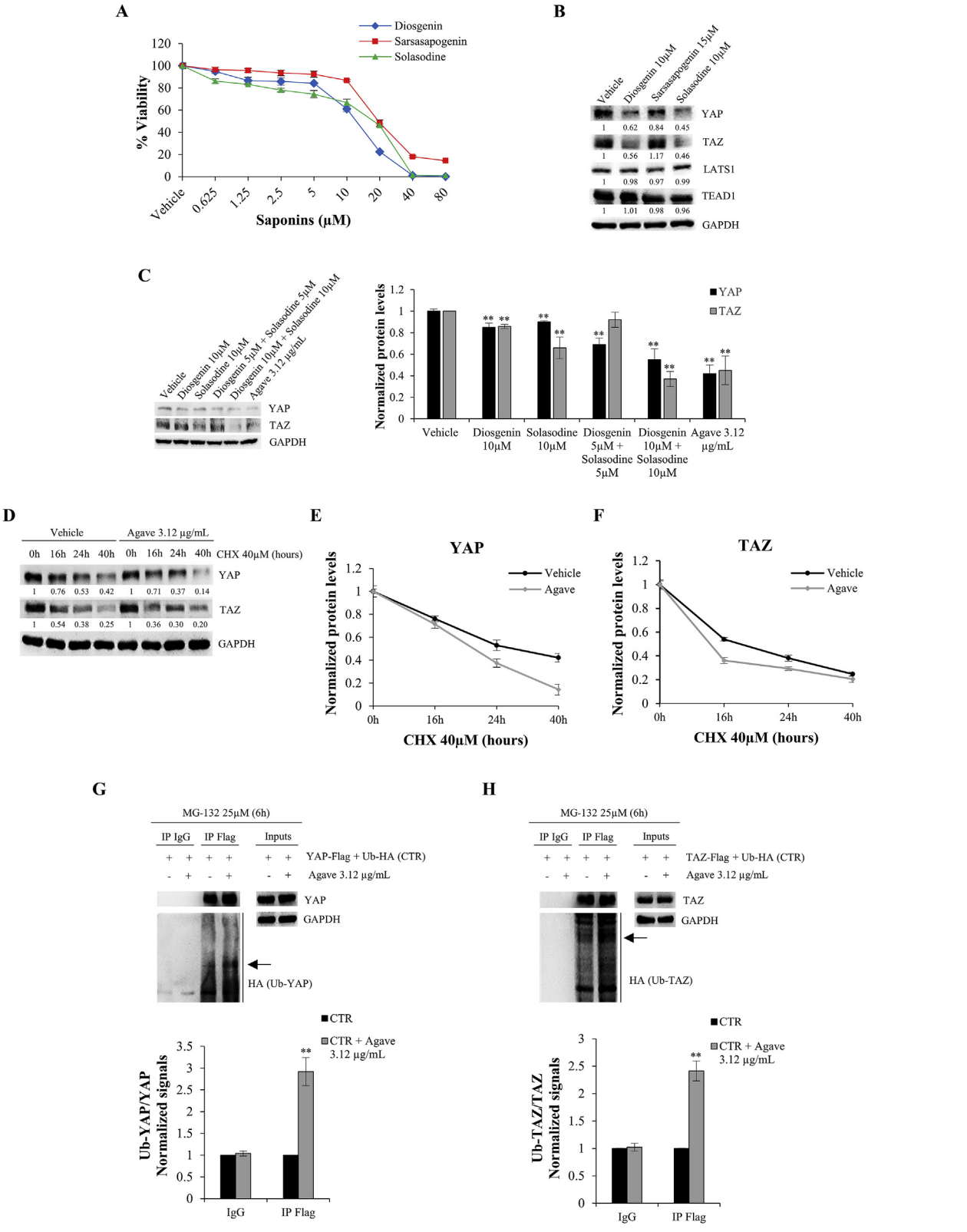

(caption on next page)

3.3. Saponins in Agave extract down-regulate YAP and TAZ protein levels

To dissect the molecular mechanism by which Agave extract functions, we investigated the effect of saponins, which are the most abundant compounds present in Agave natural extract among that with recognised anticancer effects (Supplementary Table S1) [29,30]. We assayed Diosgenin, Sarsasapogenin and Solasodine synthetic steroidal saponins using viability assays (Fig. 4A and Table 7), then treated cells with sub-lethal doses of each compound to test their effect on YAP and TAZ. Although less effective when compared to Agave, Diosgenin and Solasodine reduced both YAP and TAZ protein abundance, whilst Sarsasapogenin significantly reduced YAP at the selected concentrations

Fig. 4. Agave induces YAP and TAZ protein degradation. **(A)** U-2 OS cells were treated with Vehicle (EtOH) or increasing concentrations of Diosgenin, Sarsasapogenin and Solasodine synthetic saponins for 72 h before being analyzed by ATPlite assay. The percentage cell viability normalized to control is shown, with values representing mean ± STDEV of n = 3 independent experiments. **(B)** U-2 OS cells were treated with Vehicle, Diosgenin (10 μM), Sarsasapogenin (15 μM) or Solasodine (10 μM) for 72 h before being subjected to Western Blot analysis as indicated. GAPDH was used as a loading control. Numbers underneath immunoblots represent normalized protein amount quantified using Alliance (UVITEC) Software. Values shown are representative from n = 3 independent experiments. **(C)** U-2 OS cells were treated with Vehicle (EtOH), saponins alone or in combined treatments, or Agave extract as indicated for 72 h before being subjected to Western Blot analysis. GAPDH was used as a loading control. Histograms represent normalized protein amount quantified using Alliance (UVITEC) Software. Values shown are representative from n = 3 independent experiments, ANOVA **p < 0.001. **(D)** U-2 OS cells were treated with Vehicle or Agave (3.12 μg/mL) in combination with cycloheximide (CHX, 40 μM) for 16, 24 or 40 h, or DMSO (0 h). Cell extracts were then subjected to Western Blotting with the indicated antibodies and quantified using Alliance (UVITEC) Software. The quantitated protein level at each time point for YAP **(E)** and TAZ **(F)** was normalized to that of GAPDH. U-2 OS cells were co-transfected with Flag-tagged YAP **(G)** or TAZ **(H)** as well as HA-tagged Ubiquitin before being treated with Vehicle or Agave (3.12 μg/mL) in combination with MG-132 (25 μM) for 6 h. Protein lysates were then subjected to immunoprecipitation using anti-IgG or anti-Flag antibodies. Inputs recovered from anti-IgG IPs were loaded onto gels and subjected to immunoblot together with IP samples. Arrows indicate ubiquitinated proteins. Histograms underneath immunoblots (G–H) show ubiquitinated proteins normalized to each IP signal. Quantification was performed using Alliance (UVITEC) Software. Values represent mean ± STDEV of n = 3 independent experiments, ANOVA **p < 0.001.

Table 7
Saponins treatment reduces osteosarcoma cell viability. The half-maximal effective concentration (EC50) and the half-maximal lethal concentration (LC50) values for U-2 OS cells treated with synthetic saponins Diosgenin, Sarsasapogenin and Solasodine, calculated using Compusyn software from the dose-response curves in Fig. 4A.

Synthetic compounds	EC50 (μM)	LC50 (μM)
Diosgenin	15.93	12.5
Sarsasapogenin	29.29	20
Solasodine	4.4	17.5

(Fig. 4B). Lats1 and TEAD1 down-regulation were not observed (Fig. 4B). Interestingly, Diosgenin and Solasodine combined treatments induced a synergistic down-regulation of YAP and TAZ proteins to a similar extent of Agave (Fig. 4C).

3.4. Agave enhances YAP and TAZ protein degradation as an early event

To investigate how Agave can modulate YAP and TAZ protein levels we performed protein stability assays by treating cells with cycloheximide (CHX) in the presence or absence of Agave, then harvesting cells at different time points. Agave treatment resulted in significantly reduced YAP and TAZ protein levels at 24 and 16 h, respectively (Fig. 4D–F). Agave-induced YAP/TAZ reduction was mediated by ubiquitin-dependent proteasomal degradation as indicated by the increased abundance of ubiquitinated YAP/TAZ (Fig. 4G–H). The rapid loss of YAP and TAZ proteins suggests that ubiquitin-mediated YAP/TAZ degradation is an early event following Agave administration.

3.5. Agave reduces YAP and TAZ mRNA as a late event

In addition to decreasing YAP/TAZ protein abundance, we investigated whether Agave reduces *YAP* and *TAZ* mRNA expression. Treatment with Agave for 72 h resulted in a significant decrease in *YAP* (2.3-fold, $p < 0.001$) and *TAZ* (1.9-fold, $p < 0.001$) mRNA (Fig. 5A–B). This reduced the ability of YAP and TAZ to function as transcriptional co-activators since the expression of their target genes: *Connective Tissue Growth Factor* (*CTGF*), *Ankyrin Repeat Domain-containing protein 1 (ANKRD1)* and *Minichromosome maintenance Complex component 7 (MCM7)* were also significantly down-regulated (Fig. 5C–E). Interestingly, treatment with CDDP alone decreased *YAP* and *TAZ* expression, as well as their transcriptional function (determined by target gene expression) by 96 h (Fig. 5A–E). This is consistent with the results showed in Fig. 2C in which CDPP alone did not modulate YAP and TAZ protein levels after 72 h of treatment. Importantly however, the observed effect was less than for Agave either alone or in combination with CDDP (Fig. 5A–E). *TEAD1* mRNA was slightly decreased (1.2 fold, $p < 0.01$) after 72 h of Agave or CDDP treatment (Supplementary Fig. S2F), suggesting non-specific regulation. *LATS1* and *LATS2* were not affected by any treatment (Supplementary Figs. S2G–H).

3.6. Agave down-regulates YAP and TAZ mRNA by inhibiting NF-κB transcriptional activator function

To investigate the observed transcriptional inhibition mediated by Agave, we analyzed the promoter sequence of YAP and TAZ for transcription factor binding sites using LASAGNA-Search 2.0. Notably, we found multiple consensus binding sites for NF-κB p65/p50 homo- and hetero-dimers within YAP (Supplementary Fig. S2I) and TAZ (Supplementary Fig. S2J) promoters. This was very intriguing because NF-κB transcription factors play an oncogenic role in various cancers and have been shown to promote metastasis and chemoresistance in OS [3,31,32].

To determine whether the NF-κB consensus-binding sites identified within the YAP and TAZ promoters are linked to their transcriptional regulation by Agave, we performed ChIP analysis using NF-κB p65 and p50 subunits, and p300 histone acetyltransferase as control of transcriptionally active chromatin for two (YAP) and three (TAZ) predicted sites (Fig. 6A). Using the H1H2BA sequence as a non-modulated control (Fig. 6B), we observed that treatment with Agave decreased NF-κB p65/p50 recruitment to YAP's first putative binding site (Fig. 6C), and reduced p65 recruitment, whilst simultaneously increasing p50 binding, at YAP's second binding site (Fig. 6D). Agave treatment reduced p300 histone acetylase recruitment to both YAP binding sites (Fig. 6C–D), indicating impairment of YAP transcription. Similarly, Agave reduced NF-κB p65/p50 and p300 recruitment to all three TAZ binding sites (Fig. 6E–G). Of particular note, TAZ's first binding site was strongly regulated by NF-κB p65:p65 homo-dimers, and Agave treatment abolished this recruitment (Fig. 6E).

Since NF-κB transcription factors bind to and regulate YAP and TAZ transcription (Fig. 6), we subsequently investigated whether Agave regulates NF-κB protein expression. Treatment of U-2 OS cells with Agave for 48 h resulted in significant accumulation of NF-κB p50, and a slight decrease of NF-κB p65 (Fig. 7A). Treatment of Saos-2, MG-63 and HOS cell lines showed a consistent pattern of p65 and p50 expression after 72 h (Fig. 7B). As described previously, NF-κB functions as dimers to either activate (p65:p65 and p65:p50) or repress (p50:p50) gene transcription [15]. In addition to total abundance, the relative ratio of different subunits determines the outcome of NF-κB signalling [15]. Quantitation of p65/p50 protein ratios revealed that Agave treatment strongly favours the accumulation of NF-κB inhibitory subunit p50 in all tested cell lines (Fig. 7C).

NF-κB dimers need to be localized to the nucleus to exert their transcriptional effect. We thus investigated the sub-cellular localization of NF-κB subunits following Agave treatment using nuclear/cytoplasmic fractionation. Agave treatment increased nuclear accumulation of p105 (p50 precursor) and p50, and simultaneously reduced p65 localization to the nucleus (Fig. 7D–E). These data are consistent with

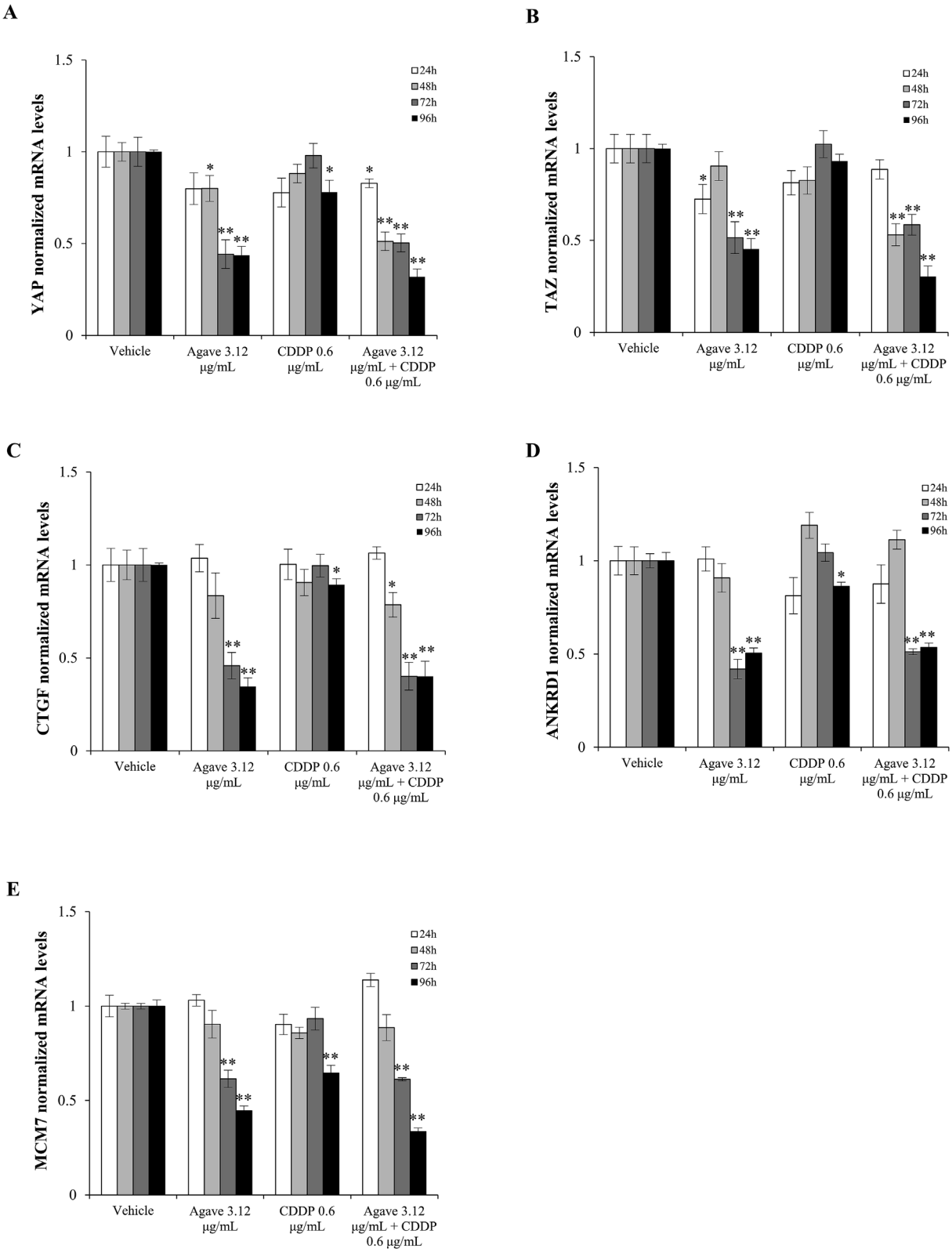

Fig. 5. Agave transcriptionally down-regulates YAP and TAZ. U-2 OS cells were treated with Vehicle (EtOH), Agave (3.12 µg/mL), and/or CDDP (0.6 µg/mL) for the indicated times before being subjected to Real Time qPCR analysis. Histograms show the mean ± STDEV mRNA level of YAP **(A)**, TAZ **(B)**, CTGF **(C)**, ANKRD1 **(D)**, and MCM7 **(E)** normalized to GAPDH (n = 3), ANOVA *p < 0.01 **p < 0.001.

immunofluorescent staining for NF-κB p105/p50 in the absence and presence of IL-6 (to activate NF-κB signalling) (Fig. 7F–G), and NF-κB p65 (Fig. 7H–I), following treatment with Agave. Finally, consistent with the altered expression and localization of NF-κB subunits induced by Agave, the expression of various NF-κB target genes was significantly reduced (Fig. 7J).

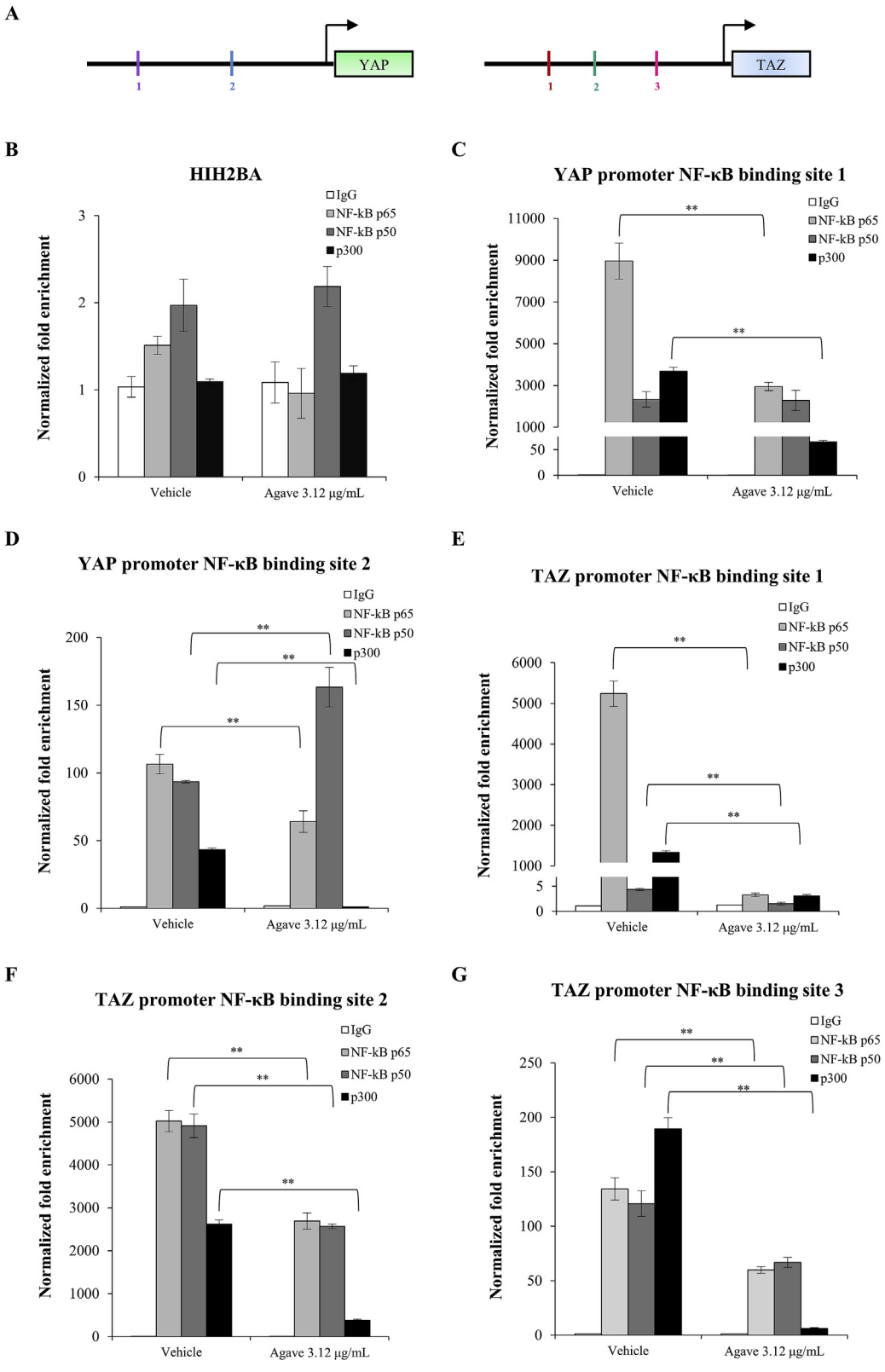

Fig. 6. Agave inhibits NF-κB recruitment onto YAP and TAZ promoters. **(A)** Schematic representation of the relative position of the putative NF-κB binding sites within the YAP and TAZ promoters. Different sites are highlighted in different colors, which are consistent with that used for sequences showed in Supplementary Figs. S2I–J. U-2 OS cells were treated with Vehicle (EtOH) or Agave (3.12 µg/mL) for 72 h before being analyzed by ChIP. Samples were immunoprecipitated with antibodies against IgG, NF-κB p65, NF-κB p50 or p300 and then subjected to qPCR analysis. Histograms shows the mean fold enrichment ± STDEV (n = 3) for H1H2BA **(B)**, and the putative NF-κB binding sites within the YAP **(C–D)** and TAZ **(E–G)** promoters, ANOVA **p < 0.001. (For interpretation of the references to color in this figure legend, the reader is referred to the Web version of this article.)

4. Discussion

Agave natural extract is known to exert prebiotic and immunomodulatory effects, as well as putative anticancer activity in colorectal and cervical cancer cells [33–35]. Here, we tested the antitumorigenic potential of Agave in OS cell lines, demonstrating that it can reduce cell viability, impair migration and colony formation, and can sensitize cells to CDDP and radiation therapies. We found that conventional chemotherapeutic drugs can induce YAP and TAZ protein expression. This might lead to YAP/TAZ-mediated increased chemoresistance of OS cells. This effect is minimized in the presence of Agave due to its ability to significantly downregulate YAP and TAZ protein expression. Indeed, Agave treatment down-regulates YAP and TAZ protein expression while direct silencing of YAP/TAZ in OS lines

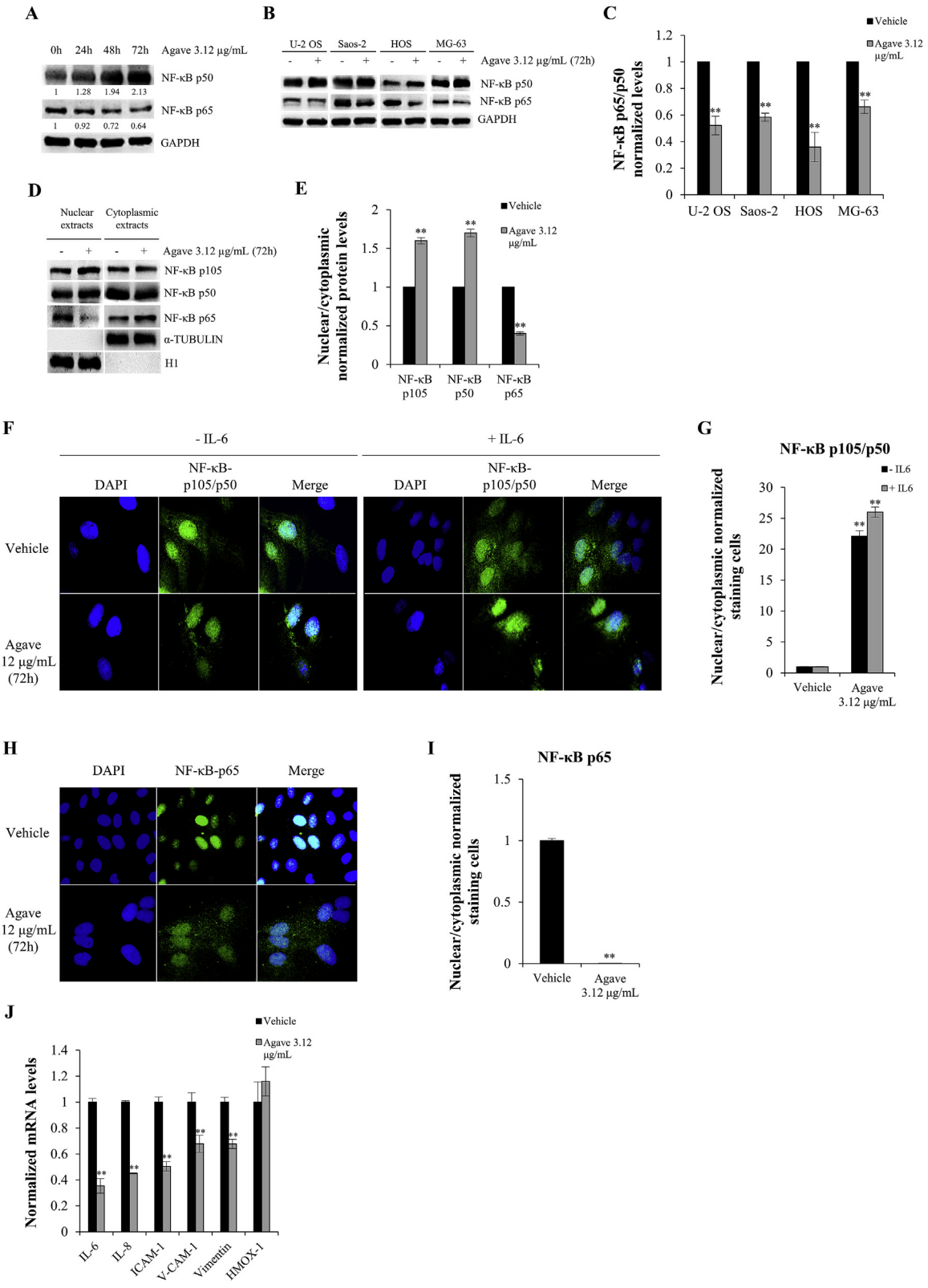

(caption on next page)

reduced cell survival, colony formation and migration capability. Consistently with a previous publication, Agave-induced apoptosis occurs irrespective to *TP53* status [35].

Our findings support that of multiple reports, identifying an oncogenic role for YAP and TAZ in OS [4,7]. YAP/TAZ are frequently overexpressed in human OS samples, correlating with target gene expression, OS staging and overall patient survival [4,36]. Further, YAP suppression impairs OS cell proliferation and migration *in vitro*, and reduces tumor growth *in vivo* [4]. Mechanistically, up-regulation of YAP in osteo-tissues is mediated by Sox2 inhibition of NF2 and Kibra, which are activators of the Hippo pathway [37], and by activation of Hedgehog signalling via Hippo pathway crosstalk [4]. In addition,

Fig. 7. Agave down-regulates NF-κB transcriptional function. **(A)** U-2 OS cells were treated with Agave (3.12 μg/mL) for 24, 48 or 72 h, or EtOH as Vehicle control (0 h), then subjected to Western Blot analysis as indicated. GAPDH was used as a loading control. Numbers underneath immunoblots represent normalized protein amount quantified using Alliance (UVITEC) Software. Values shown are representative from n = 3 independent experiments. **(B)** U-2 OS, Saos-2, HOS and MG-63 cells were treated with Agave (3.12 μg/mL) or Vehicle for 72 h before being subjected to Western Blot analysis. The abundance of NF-κB p65 and NF-κB p50 was quantified using Alliance (UVITEC) Software and the NF-κB p65/p50 ratio was determined. The relative ratios are shown in **(C)**. Values represent mean ± STDEV (n = 3), with U-2 OS cells treated with Vehicle normalized to 1, **p < 0.001. **(D)** U-2 OS cells were treated with Vehicle or Agave (3.12 μg/mL) for 72 h before being subjected to nuclear/cytoplasmic fractionation followed by Western Blot analysis. H1 (nuclear) and α-Tubulin (cytoplasmic) were used as loading controls. The nuclear/cytoplasmic ratios for NF-κB p105, p50 and p65 were determined **(E)**. Values represent mean ± STDEV (n = 3), with U-2 OS cells treated with Vehicle normalized to 1, ANOVA **p < 0.001. **(F, H)** U-2 OS cells were treated with Vehicle or Agave (3.12 μg/mL) either in the absence or presence of IL-6 (100 ng/mL) for 72 h. Cells were then stained for NF-κB p105/p50 (F), or p65 (H) with nuclei marked by DAPI staining. Nuclear and cytoplasmic signal was quantified using ImageJ software, and the relative mean ± STDEV for NF-κB p105/p50 **(G)** and NF-κB p65 **(I)** is shown, with cells treated with Vehicle normalized to 1, n = 3 ANOVA **p < 0.001. **(J)** U-2 OS cells were treated with Vehicle or Agave (3.12 μg/mL) for 72 h before being subjected to Real Time qPCR analysis. The mean mRNA level ± STDEV (n = 3) for each target gene is shown, with cells treated with Vehicle normalized to 1, ANOVA **p < 0.001.

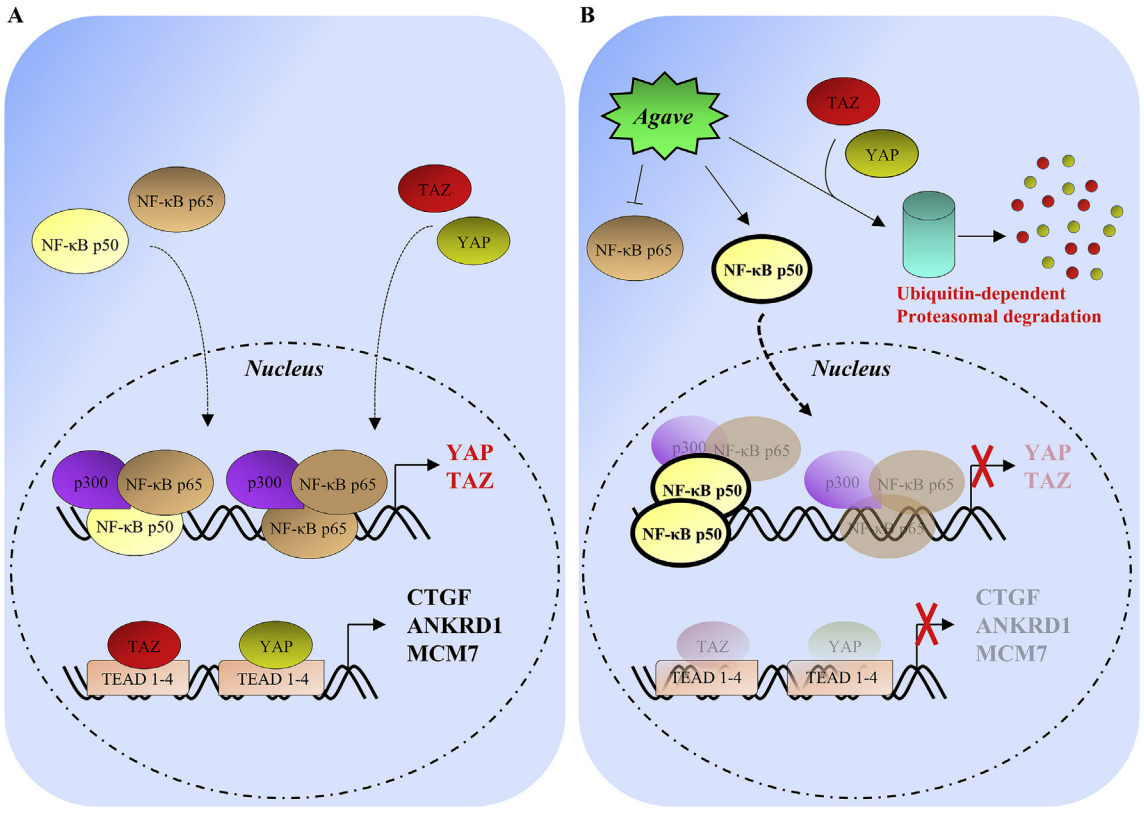

Fig. 8. Proposed model of Agave's anticancer activity in osteosarcoma. **(A)** NF-κB p65:p50 and/or NF-κB p65:p65 dimers bind to YAP and TAZ promoters inducing p300 recruitment and transcriptional activation. YAP and TAZ activated proteins, translocate into the nucleus to activate transcription of oncogenic targets genes *CTGF*, *ANKRD1* and *MCM7*. **(B)** Agave treatment promotes YAP/TAZ ubiquitin-dependent proteasomal degradation, reducing their nuclear translocation. Moreover, Agave down-regulates NF-κB p65 and promotes its cytoplasmic sequestration, whereas NF-κB p50 is up-regulated and enriched in the nuclear compartment. YAP and TAZ transcription is therefore strongly diminished, as is their downstream targets.

RASSFs, NF2 and Mob1 tumor suppressor proteins are frequently mutated in OS, resulting in increased YAP and TAZ activation [4]. Importantly, there is good evidence for the involvement of YAP/TAZ in inducing chemo-, radio- and molecular targeted therapy-resistant OS [7,38].

Agave extract is a complex blend of compounds amongst which sapogenins and saponins stand out as bioactive components with multiple functions. Unlike Agave, which is poorly studied, saponins have been widely investigated, with numerous reports citing their antimicrobial [39], pro-apoptotic [40], immunomodulatory [41], neuroprotective [42], anti-proliferative [30] and anti-migratory properties in various cancer cell lines [43–45]. At high doses (> 100 μM), saponins exert a cytotoxic effect by disrupting cell membranes. At low doses however, they induce apoptosis by multiple mechanisms including activation of Tumor Necrosis Factor-Receptor (TNF-R) and FAS-L receptors, cleavage of Caspase 3 and 9, and induction of p53 by inhibiting Mouse Double Minute 2 homolog (Mdm2) [46–49]. They also block cell proliferation [50,51], impair migration and EMT [29], and regulate various signalling pathways including PI3K/Akt, MAPK and NF-κB [52–56]. Consistent with saponins' tumor suppressive properties, we demonstrate that synthetic saponins reduce cell viability, and down-regulate YAP/TAZ abundance, although to a lesser extent than Agave itself. Nevertheless, combined treatments of saponins show a synergistic effect recapitulating YAP and TAZ down-regulation mediated by Agave treatments. This is consistent with previous reports demonstrating that the anti-inflammatory properties of Agave extract, mediated by NF-κB modulation, could be partially recapitulated by saponins [57–59]. In detail, saponins reduce NF-κB activity and its binding to DNA either by preventing IκB degradation [57,58], or increasing SIRT1 levels, resulting in reduced NF-κB p65 acetylation and subsequent transcriptional activation [59]. This might be the mechanism of Agave's action on NF-κB in this study. However, due to the complexity of Agave extract, it is likely that a combination of active components could activate/inhibit multiple signalling pathways simultaneously, to produce a

greater overall effect.

We propose that Agave initially induces YAP and TAZ protein destabilization by promoting ubiquitin-dependent proteasomal degradation. Subsequently, Agave impairs YAP and TAZ transcription by regulating NF-κB expression, and consequently NF-κB subunit recruitment to YAP and TAZ promoter sequences. Indeed, we suggest for the first time that NF-κB subunits bind directly to YAP/TAZ promoters to activate their transcription.

We considered that Agave's modulation of NF-κB could directly regulate apoptosis and chemosensitivity, bypassing YAP/TAZ transcriptional regulation [3,15]. Saponins cooperate with CDDP to induce reactive oxygen species production, resulting in apoptosis [29]. Chemical inhibitors of NF-κB (parthenolide and BRM270) sensitize OS to chemo- and radio-therapies, and activate apoptosis [60–62]. Moreover, NF-κB inhibition can sensitize cells to chemotherapeutics via up-regulation of IL-6, an activator of NF-κB signalling [60].

Data presented here, indicate that YAP/TAZ as well as NF-κB are mediators of Agave-induced anti-proliferative, anti-migratory and pro-apoptotic effects in OS cell lines, and possibly in OS of animals and human patients. We show that Agave induces YAP/TAZ protein degradation as an early event, and subsequently impairs YAP and TAZ transcription by inactivating NF-κB (Fig. 8). We propose that Agave-mediated YAP/TAZ down-regulation and NF-κB inactivation result in a pro-apoptotic, anti-migratory phenotype with enhanced chemo- and radio-sensitivity. OS could therefore potentially be targeted by drugs that have recently emerged as inhibitors of the critical YAP/TAZ-TEAD complexes, which drive transcription of proliferative and anti-apoptotic genes. Among YAP/TAZ inhibitors, verteporfin was shown to inhibit YAP-induced overgrowth of liver in animal models [27]. Translocation of YAP/TAZ to the nucleus was shown to be blocked by two FDA-approved tyrosine kinase inhibitors, dasatinib and pazopanib [28], and the egress of YAP from the nucleus was facilitated by dobutamine, sympathomimetic drug used in the treatment of heart failure [63]. Here we show that verteporfin, dasatinib and pazopanib reduce OS cell viability in a dose-dependent manner. These results highlight that YAP and TAZ exert a key oncogenic pro-survival role in osteosarcoma and suggest that YAP and TAZ inhibition could be a promising strategy for treating osteosarcoma. It is anticipated that new therapeutic compounds that inhibit YAP/TAZ-TEAD will emerge soon. Natural compounds offer advantages over traditional chemotherapies as they typically exhibit low toxicity, are associated with low production costs, and offer the potential for multi-faceted mechanisms of action. Such new drugs for YAP/TAZ could be complemented with selected saponins of Agave to better control and manage OS. Agave/saponin-mediated NF-κB inactivation could be of interest for the treatment of other tumours in which NF-κB is known to play an oncogenic role, including myeloid malignancies [64], breast [65], lung [66], liver [67] and ovarian [68] cancers. Similarly, for tumours in which YAP/TAZ play critical oncogenic roles [12,69]. We advocate that Agave natural extract is a promising agent to treat OS, either independently, or as an adjuvant to reduce the intrinsic toxic side effects of chemotherapeutics.

Conflicts of interest

The authors declare no conflict of interest.

Acknowledgements

We greatly thank the financial support of the Italian Association for Cancer Research (Grant n. 20613) and of the Epigenomics Flagship Project (EPIGEN; sub-project 7.6) to G.B., of the Aboca (S.P.A) to S.S, of the AIRC-FIRC Fellowship (ID. 19371) and of “Associazione Aurora Tomaselli Ricerca e Prevenzione” to M.F. E.K. is supported from the Aboca (S.P.A). We wish to thank Aurora Tomaselli Association for proposing originally this work to us.

Appendix A. Supplementary data

Supplementary data related to this article can be found at http://dx.doi.org/10.1016/j.canlet.2018.06.021.

References

[1] A. Alfranca, L. Martinez-Cruzado, J. Tornin, A. Abarrategi, T. Amaral, E. de Alava, P. Menendez, J. Garcia-Castro, R. Rodriguez, Bone microenvironment signals in osteosarcoma development, Cell. Mol. Life Sci.: CMLS 72 (2015) 3097–3113.
[2] A.E. Rosenberg, WHO Classification of Soft Tissue and Bone, fourth edition: summary and commentary, Curr. Opin. Oncol. 25 (2013) 571–573.
[3] A. Abarrategi, J. Tornin, L. Martinez-Cruzado, A. Hamilton, E. Martinez-Campos, J.P. Rodrigo, M.V. Gonzalez, N. Baldini, J. Garcia-Castro, R. Rodriguez, Osteosarcoma: cells-of-origin, cancer stem cells, and targeted therapies, Stem Cells International 2016 (2016) 3631764.
[4] M.D. Deel, J.J. Li, L.E. Crose, C.M. Linardic, A review: molecular aberrations within hippo signaling in bone and soft-tissue sarcomas, Frontiers in oncology 5 (2015) 190.
[5] S.M. Botter, D. Neri, B. Fuchs, Recent advances in osteosarcoma, Curr. Opin. Pharmacol. 16 (2014) 15–23.
[6] D.J. Harrison, C.L. Schwartz, Osteogenic sarcoma: systemic chemotherapy options for localized disease, Curr. Treat. Options Oncol. 18 (2017) 24.
[7] D.Y. Wang, Y.N. Wu, J.Q. Huang, W. Wang, M. Xu, J.P. Jia, G. Han, B.B. Mao, W.Z. Bi, Hippo/YAP signaling pathway is involved in osteosarcoma chemoresistance, Chin. J. Canc. 35 (2016) 47.
[8] D.C. Allison, S.C. Carney, E.R. Ahlmann, A. Hendifar, S. Chawla, A. Fedenko, C. Angeles, L.R. Menendez, A meta-analysis of osteosarcoma outcomes in the modern medical era, Sarcoma 2012 (2012) 704872.
[9] X. He, Z. Gao, H. Xu, Z. Zhang, P. Fu, A meta-analysis of randomized control trials of surgical methods with osteosarcoma outcomes, J. Orthop. Surg. Res. 12 (2017) 5.
[10] M.S. Ferraiuolo, G. Blandino, The hippo pathway, in: R.A.B.a.P.D. Stahl (Ed.), Encyclopedia of Cell Biology, Academic Press, Waltham, MA, 2016, pp. 99–106.
[11] Y. Wang, A. Yu, F.X. Yu, The Hippo pathway in tissue homeostasis and regeneration, Protein & cell 8 (5) (2017) 349–359.
[12] F. Zanconato, M. Cordenonsi, S. Piccolo, YAP/TAZ at the roots of cancer, Canc. Cell 29 (2016) 783–803.
[13] B. Zhao, L. Li, L. Wang, C.Y. Wang, J. Yu, K.L. Guan, Cell detachment activates the Hippo pathway via cytoskeleton reorganization to induce anoikis, Genes Dev. 26 (2012) 54–68.
[14] M. Ferraiuolo, L. Verduci, G. Blandino, S. Strano, Mutant p53 protein and the hippo transducers YAP and TAZ: a critical oncogenic node in human cancers, Int. J. Mol. Sci. 18 (2017).
[15] S. Mitchell, J. Vargas, A. Hoffmann, Signaling via the NFkappaB system, Wiley interdisciplinary reviews, Systems biology and medicine 8 (2016) 227–241.
[16] M. Pasello, F. Michelacci, I. Scionti, C.M. Hattinger, M. Zuntini, A.M. Caccuri, K. Scotlandi, P. Picci, M. Serra, Overcoming glutathione S-transferase P1-related cisplatin resistance in osteosarcoma, Canc. Res. 68 (2008) 6661–6668.
[17] C. Pulito, F. Mori, A. Sacconi, L. Casadei, M. Ferraiuolo, M.C. Valerio, R. Santoro, F. Goeman, A. Maidecchi, L. Mattoli, C. Manetti, S. Di Agostino, P. Muti, G. Blandino, S. Strano, Cynara scolymus affects malignant pleural mesothelioma by promoting apoptosis and restraining invasion, Oncotarget 6 (2015) 18134–18150.
[18] S. Di Agostino, S. Strano, V. Emiliozzi, V. Zerbini, M. Mottolese, A. Sacchi, G. Blandino, G. Piaggio, Gain of function of mutant p53: the mutant p53/NF-Y protein complex reveals an aberrant transcriptional mechanism of cell cycle regulation, Canc. Cell 10 (2006) 191–202.
[19] F. Fausti, S. Di Agostino, M. Cioce, P. Bielli, C. Sette, P.P. Pandolfi, M. Oren, M. Sudol, S. Strano, G. Blandino, ATM kinase enables the functional axis of YAP, PML and p53 to ameliorate loss of Werner protein-mediated oncogenic senescence, Cell Death and Differentiation 20 (2013) 1498–1509.
[20] S. Di Agostino, G. Sorrentino, E. Ingallina, F. Valenti, M. Ferraiuolo, S. Bicciato, S. Piazza, S. Strano, G. Del Sal, G. Blandino, YAP enhances the pro-proliferative transcriptional activity of mutant p53 proteins, EMBO Reports 17 (2016) 188–201.
[21] M. Gordon, M. El-Kalla, Y. Zhao, Y. Fiteih, J. Law, N. Volodko, A. Anwar-Mohamed, A.O. El-Kadi, L. Liu, J. Odenbach, A. Thiesen, C. Onyskiw, H.A. Ghazaleh, J. Park, S.B. Lee, V.C. Yu, C. Fernandez-Patron, R.T. Alexander, E. Wine, S. Baksh, The tumor suppressor gene, RASSF1A, is essential for protection against inflammation -induced injury, PLoS One 8 (2013) e75483.
[22] L. Azzolin, F. Zanconato, S. Bresolin, M. Forcato, G. Basso, S. Bicciato, M. Cordenonsi, S. Piccolo, Role of TAZ as mediator of Wnt signaling, Cell 151 (2012) 1443–1456.
[23] M. Muscolini, E. Montagni, V. Palermo, S. Di Agostino, W. Gu, S. Abdelmoula-Souissi, C. Mazzoni, G. Blandino, L. Tuosto, The cancer-associated K351N mutation affects the ubiquitination and the translocation to mitochondria of p53 protein, J. Biol. Chem. 286 (2011) 39693–39702.
[24] C. Pulito, F. Mori, A. Sacconi, F. Goeman, M. Ferraiuolo, P. Pasanisi, C. Campagnoli, F. Berrino, M. Fanciulli, R.J. Ford, M. Levrero, N. Pediconi, L. Ciuffreda, M. Milella, G.R. Steinberg, M. Cioce, P. Muti, S. Strano, G. Blandino, Metformin-induced ablation of microRNA 21-5p releases Sestrin-1 and CAB39L antitumoral activities, Cell discovery 3 (2017) 17022.
[25] F. Mori, M. Ferraiuolo, R. Santoro, A. Sacconi, F. Goeman, M. Pallocca, C. Pulito, E. Korita, M. Fanciulli, P. Muti, G. Blandino, S. Strano, Multitargeting activity of miR-24 inhibits long-term melatonin anticancer effects, Oncotarget 7 (2016) 20532–20548.

[26] L. Verduci, M. Ferraiuolo, A. Sacconi, F. Ganci, J. Vitale, T. Colombo, P. Paci, S. Strano, G. Macino, N. Rajewsky, G. Blandino, The oncogenic role of circPVT1 in head and neck squamous cell carcinoma is mediated through the mutant p53/YAP/TEAD transcription-competent complex, Genome Biol. 18 (2017) 237.
[27] Y. Liu-Chittenden, B. Huang, J.S. Shim, Q. Chen, S.J. Lee, R.A. Anders, J.O. Liu, D. Pan, Genetic and pharmacological disruption of the TEAD-YAP complex suppresses the oncogenic activity of YAP, Genes Dev. 26 (2012) 1300–1305.
[28] Y. Oku, N. Nishiya, T. Shito, R. Yamamoto, Y. Yamamoto, C. Oyama, Y. Uehara, Small molecules inhibiting the nuclear localization of YAP/TAZ for chemotherapeutics and chemosensitizers against breast cancers, FEBS open bio 5 (2015) 542–549.
[29] P. Koczurkiewicz, J. Czyz, I. Podolak, K. Wojcik, A. Galanty, Z. Janeczko, M. Michalik, Multidirectional effects of triterpene saponins on cancer cells - mini-review of in vitro studies, Acta Biochimica Polonica 62 (2015) 383–393.
[30] J. Sidana, B. Singh, O.P. Sharma, Saponins of Agave: chemistry and bioactivity, Phytochemistry 130 (2016) 22–46.
[31] J. Inoue, J. Gohda, T. Akiyama, K. Semba, NF-kappaB activation in development and progression of cancer, Canc. Sci. 98 (2007) 268–274.
[32] X.M. Xu, W. Liu, Z.H. Cao, M.X. Liu, Effects of ZEB1 on regulating osteosarcoma cells via NF-kappaB/iNOS, Eur. Rev. Med. Pharmacol. Sci. 21 (2017) 1184–1190.
[33] P. Allsopp, S. Possemiers, D. Campbell, I.S. Oyarzabal, C. Gill, I. Rowland, An exploratory study into the putative prebiotic activity of fructans isolated from Agave angustifolia and the associated anticancer activity, Anaerobe 22 (2013) 38–44.
[34] J.M. Gutierrez-Hernandez, A. Escalante, R.N. Murillo-Vazquez, E. Delgado, F.J. Gonzalez, G. Toriz, Use of Agave tequilana-lignin and zinc oxide nanoparticles for skin photoprotection, J. Photochem. Photobiol. B Biol. 163 (2016) 156–161.
[35] N.N. Mthembu, L.R. Motadi, Apoptotic potential role of Agave palmeri and Tulbaghia violacea extracts in cervical cancer cells, Mol. Biol. Rep. 41 (2014) 6143–6155.
[36] C. Bouvier, N. Macagno, Q. Nguyen, A. Loundou, C. Jiguet-Jiglaire, J.C. Gentet, J.L. Jouve, A. Rochwerger, J.C. Mattei, D. Bouvard, S. Salas, Prognostic value of the hippo pathway transcriptional coactivators YAP/TAZ and beta1-integrin in conventional osteosarcoma, Oncotarget 7 (40) (2016) 64702–64710.
[37] E. Seo, U. Basu-Roy, P.H. Gunaratne, C. Coarfa, D.S. Lim, C. Basilico, A. Mansukhani, SOX2 regulates YAP1 to maintain stemness and determine cell fate in the osteo-adipo lineage, Cell Reports 3 (2013) 2075–2087.
[38] M.H. Kim, J. Kim, Role of YAP/TAZ transcriptional regulators in resistance to anticancer therapies, Cell. Mol. Life Sci.: CMLS 74 (2017) 1457–1474.
[39] H.J. Li, M.B. Foston, R. Kumar, R. Samuel, X.D. Gao, F. Hu, A.J. Ragauskas, C.E. Wyman, Chemical composition and characterization of cellulose for Agave as a fast-growing, drought-tolerant biofuels feedstock, RSC Adv. 2 (2012) 4951–4958.
[40] P.Y. Chen, C.H. Chen, C.C. Kuo, T.H. Lee, Y.H. Kuo, C.K. Lee, Cytotoxic steroidal saponins from Agave sisalana, Planta Medica 77 (2011) 929–933.
[41] T. Uemura, S. Hirai, N. Mizoguchi, T. Goto, J.Y. Lee, K. Taketani, Y. Nakano, J. Shono, S. Hoshino, N. Tsuge, T. Narukami, N. Takahashi, T. Kawada, Diosgenin present in fenugreek improves glucose metabolism by promoting adipocyte differentiation and inhibiting inflammation in adipose tissues, Mol. Nutr. Food Res. 54 (2010) 1596–1608.
[42] A. Sun, X. Xu, J. Lin, X. Cui, R. Xu, Neuroprotection by saponins, Phytother Res.: PTR 29 (2015) 187–200.
[43] A.M. Leal-Diaz, L.G. Noriega, I. Torre-Villalvazo, N. Torres, G. Aleman-Escondrillas, P. Lopez-Romero, M. Sanchez-Tapia, M. Aguilar-Lopez, J. Furuzawa-Carballeda, L.A. Velazquez-Villegas, A. Avila-Nava, G. Ordaz, J.A. Gutierrez-Uribe, S.O. Serna-Saldivar, A.R. Tovar, Aguamiel concentrate from Agave salmiana and its extracted saponins attenuated obesity and hepatic steatosis and increased Akkermansia muciniphila in C57BL6 mice, Sci. Rep. 6 (2016) 34242.
[44] S. Man, W. Gao, Y. Zhang, L. Huang, C. Liu, Chemical study and medical application of saponins as anti-cancer agents, Fitoterapia 81 (2010) 703–714.
[45] L. Santos-Zea, A.M. Rosas-Perez, A.M. Leal-Diaz, J.A. Gutierrez-Uribe, Variability in saponin content, cancer antiproliferative activity and physicochemical properties of concentrated Agave sap, J. Food Sci. 81 (2016) H2069–H2075.
[46] C. Corbiere, B. Liagre, F. Terro, J.L. Beneytout, Induction of antiproliferative effect by diosgenin through activation of p53, release of apoptosis-inducing factor (AIF) and modulation of caspase-3 activity in different human cancer cells, Cell Research 14 (2004) 188–196.
[47] T. Ohtsuki, T. Koyano, T. Kowithayakorn, S. Sakai, N. Kawahara, Y. Goda, N. Yamaguchi, M. Ishibashi, New chlorogenin hexasaccharide isolated from Agave fourcroydes with cytotoxic and cell cycle inhibitory activities, Bioorg. Med. Chem. 12 (2004) 3841–3845.
[48] S.B. Song, N.H. Tung, T.H. Quang, N.T. Ngan, K.E. Kim, Y.H. Kim, Inhibition of TNF-alpha-mediated NF-kappaB transcriptional activity in HepG2 cells by dammarane-type saponins from panax ginseng leaves, Journal of ginseng research 36 (2012) 146–152.
[49] P. Trouillas, C. Corbiere, B. Liagre, J.L. Duroux, J.L. Beneytout, Structure-function relationship for saponin effects on cell cycle arrest and apoptosis in the human 1547 osteosarcoma cells: a molecular modelling approach of natural molecules structurally close to diosgenin, Bioorg. Med. Chem. 13 (2005) 1141–1149.
[50] S. Moalic, B. Liagre, C. Corbiere, A. Bianchi, M. Dauca, K. Bordji, J.L. Beneytout, A plant steroid, diosgenin, induces apoptosis, cell cycle arrest and COX activity in osteosarcoma cells, FEBS Letters 506 (2001) 225–230.
[51] X. Wei, T. Shimizu, Z.C. Lai, Mob as tumor suppressor is activated by Hippo kinase for growth inhibition in Drosophila, EMBO J. 26 (2007) 1772–1781.
[52] G. Cheng, F. Gao, X. Sun, H. Bi, Y. Zhu, Paris saponin VII suppresses osteosarcoma cell migration and invasion by inhibiting MMP2/9 production via the p38 MAPK signaling pathway, Mol. Med. Rep. 14 (2016) 3199–3205.
[53] J.H. Choi, S.W. Jin, E.H. Han, B.H. Park, H.G. Kim, T. Khanal, Y.P. Hwang, M.T. Do, H.S. Lee, Y.C. Chung, H.S. Kim, T.C. Jeong, H.G. Jeong, Platycodon grandiflorum root-derived saponins attenuate atopic dermatitis-like skin lesions via suppression of NF-kappaB and STAT1 and activation of Nrf2/ARE-mediated heme oxygenase-1, Phytomed. Int. J. Phytother. Phytopharm. 21 (2014) 1053–1061.
[54] R.Y. Mohammad, G. Somayyeh, H. Gholamreza, M. Majid, R. Yousef, Diosgenin inhibits hTERT gene expression in the A549 lung cancer cell line, Asian Pac. J. Cancer Prev. APJCP 14 (2013) 6945–6948.
[55] S.C. Tseng, T.S. Shen, C.C. Wu, I.L. Chang, H.Y. Chen, C.P. Hsieh, C.H. Cheng, C.L. Chen, Methyl protodioscin induces apoptosis in human osteosarcoma cells by caspase-dependent and MAPK signaling pathways, J. Agric. Food Chem. 65 (2017) 2670–2676.
[56] H. Xiong, Y. Zheng, G. Yang, H. Wang, Z. Mei, Triterpene saponins with anti-inflammatory activity from the stems of Entada phaseoloides, Fitoterapia 103 (2015) 33–45.
[57] K.S. Ahn, E.J. Noh, H.L. Zhao, S.H. Jung, S.S. Kang, Y.S. Kim, Inhibition of inducible nitric oxide synthase and cyclooxygenase II by Platycodon grandiflorum saponins via suppression of nuclear factor-KB activation in RAW 264.7 cells, Life Sciences 76 (2005) 2315–2328.
[58] S.T. Lee, P.F. Wong, H. He, J.D. Hooper, M.R. Mustafa, Alpha-tomatine attenuation of in vivo growth of subcutaneous and orthotopic xenograft tumors of human prostate carcinoma PC-3 cells is accompanied by inactivation of nuclear factor-kappa B signaling, PLoS One 8 (2013) e57708.
[59] N. Wei, C. Zhang, H. He, T. Wang, Z. Liu, G. Liu, Z. Sun, Z. Zhou, C. Bai, D. Yuan, Protective effect of saponins extract from Panax japonicus on myocardial infarction: involvement of NF-kappaB, Sirt1 and mitogen-activated protein kinase signalling pathways and inhibition of inflammation, J. Pharm. Pharmacol. 66 (2014) 1641–1651.
[60] A.M. Castro-Gamero, K.S. Borges, V. da Silva Silveira, R.C. Lira, R. de Paula Gomes Queiroz, F.C. Valera, C.A. Scrideli, K. Umezawa, L.G. Tone, Inhibition of nuclear factor-kappaB by dehydroxymethylepoxyquinomicin induces schedule-dependent chemosensitivity to anticancer drugs and enhances chemoinduced apoptosis in osteosarcoma cells, Anti Canc. Drugs 23 (2012) 638–650.
[61] R.K. Mongre, S.S. Sodhi, M. Ghosh, J.H. Kim, N. Kim, Y.H. Park, S.J. Kim, Y.J. Heo, N. Sharma, D.K. Jeong, The novel inhibitor BRM270 downregulates tumorigenesis by suppression of NF-kappaB signaling cascade in MDR-induced stem like cancer-initiating cells, Int. J. Oncol. 46 (2015) 2573–2585.
[62] D. Zuch, A.H. Giang, Y. Shapovalov, E. Schwarz, R. Rosier, R. O'Keefe, R.A. Eliseev, Targeting radioresistant osteosarcoma cells with parthenolide, J. Cell. Biochem. 113 (2012) 1282–1291.
[63] Y. Bao, K. Nakagawa, Z. Yang, M. Ikeda, K. Withanage, M. Ishigami-Yuasa, Y. Okuno, S. Hata, H. Nishina, Y. Hata, A cell-based assay to screen stimulators of the Hippo pathway reveals the inhibitory effect of dobutamine on the YAP-dependent gene transcription, J. Biochem. 150 (2011) 199–208.
[64] D. Cilloni, G. Martinelli, F. Messa, M. Baccarani, G. Saglio, Nuclear factor kB as a target for new drug development in myeloid malignancies, Haematologica 92 (2007) 1224–1229.
[65] A. Zubair, M. Frieri, Role of nuclear factor-kB in breast and colorectal cancer, Curr. Allergy Asthma Rep. 13 (2013) 44–49.
[66] D. Wu, P. Wu, L. Zhao, L. Huang, Z. Zhang, S. Zhao, J. Huang, NF-kappab expression and outcomes in solid tumors: a systematic review and meta-analysis, Medicine 94 (2015) e1687.
[67] A. Verma, D. Singh, F. Anwar, P.C. Bhatt, F. Al-Abbasi, V. Kumar, Triterpenoids principle of Wedelia calendulacea attenuated diethynitrosamine-induced hepatocellular carcinoma via down-regulating oxidative stress, inflammation and pathology via NF-kB pathway, Inflammopharmacology 26 (1) (2017) 133–146.
[68] S. Arabzadeh, G. Hossein, Z. Salehi-Dulabi, A.H. Zarnani, WNT5A-ROR2 is induced by inflammatory mediators and is involved in the migration of human ovarian cancer cell line SKOV-3, Cell. Mol. Biol. Lett. 21 (2016) 9.
[69] K.F. Harvey, X. Zhang, D.M. Thomas, The Hippo pathway and human cancer, Nat. Rev. Canc. 13 (2013) 246–257.